



Cite this: *J. Anal. At. Spectrom.*, 2023, **38**, 827

# Rapid isotopic analysis of uranium particles by laser ablation MC-ICP-MS†

Josh Wimpenny,<sup>a</sup> Kyle M. Samperton,<sup>a</sup> Pedro Sotorrio,<sup>a</sup> Matthew S. Wellons,<sup>b</sup> Spencer M. Scott,<sup>b</sup> David Willingham<sup>a</sup> and Kim Knight<sup>a</sup>

We present a methodology for characterizing the isotopic composition of uranium (U) in  $\mu\text{m}$ -scale particles by laser ablation multicollector-inductively coupled plasma-mass spectrometry (MC-ICP-MS). Analyses were performed using two U particle materials,  $^{235}\text{U}$ -enriched Certified Reference Material (CRM) U200 and depleted uranium (DU) produced by Savannah River National Laboratory (SRNL). The laser was rastered over the sample surface and the signal derived from each individual particle was integrated separately and reduced using a bespoke data reduction package, including application of corrections for instrumental mass bias and ion counter gains. Accurate  $^{234}\text{U}/^{238}\text{U}$ ,  $^{235}\text{U}/^{238}\text{U}$  and  $^{236}\text{U}/^{238}\text{U}$  ratios were obtained with percent-level precision in samples with isotopic compositions spanning >2 orders of magnitude, including successfully resolving  $^{234}\text{U}$  and  $^{236}\text{U}$  abundances of <10 ppm and <80 ppm respectively in SRNL-DU. Comparable results obtained by laser ablation (LA) MC-ICP-MS and large geometry—secondary ionization mass spectrometry (LG-SIMS) indicate that laser ablation can provide valuable information when rapid U isotopic analysis of environmental samples is required.

Received 5th December 2022

Accepted 24th January 2023

DOI: 10.1039/d2ja00403h

rsc.li/jaas

## 1. Introduction

Environmental sampling is an International Atomic Energy Agency (IAEA) safeguards tool that helps ensure that nuclear facilities, e.g., enrichment plants, are not being misused and that there is no undeclared nuclear material contained therein. Swipe sampling is performed to collect  $\mu\text{m}$ -scale particulates which are analyzed to identify their elemental and isotopic compositions; this provides important information about the enrichment level, potential time of reprocessing, and the particle age.<sup>1</sup> The characterization of U isotope ratios in individual particles is commonly performed by large geometry—secondary ionization mass spectrometry (LG-SIMS), which can achieve a precision of <1% on the  $^{235}\text{U}/^{238}\text{U}$  ratio and <20% on the minor isotope ratios  $^{234}\text{U}/^{238}\text{U}$  and  $^{236}\text{U}/^{238}\text{U}$ .<sup>2–5</sup> However, SIMS instruments are costly, require significant investment in infrastructure and personnel, and can have strict sample preparation requirements. An alternative analytical technique that could potentially be useful for safeguards particulate analysis is laser ablation multicollector – inductively coupled plasma – mass spectrometry (MC-ICP-MS). Laser ablation is a rapid *in situ* sampling technique that requires minimal sample preparation. Modern MC-ICP-MS platforms are highly

versatile and can characterize the isotopic composition of a wide range of elements with precision down to the parts-per-million level. Thus, LA-MC-ICP-MS could potentially fill an important role as an alternative *in situ* analytical technique for isotopic analyses of U in particulate materials.

The isotopic analysis of particles by laser ablation presents several challenges in comparison with the measurement of macroscopic samples such as glasses, rock thin sections and mineral separates. First, the optics provided on most laser ablation systems are optimized for spot sizes of 10–100  $\mu\text{m}$ , which makes identifying  $\mu\text{m}$  or sub- $\mu\text{m}$  scale objects difficult. Second, the mass of material generated from ablation of a  $\mu\text{m}$ -scale particle will be orders-of-magnitude smaller than the mass generated by a typical 20–50  $\mu\text{m}$  spot analysis in glass or other solid. Thus, the resulting ion beam may not be resolvable on a Faraday detector and may be challenging to resolve using ion counters. Perhaps more significantly, any particle-scale signal that is produced will be short lived on the order of seconds, and the signal is liable to be highly unstable compared to ablation of a glass. Other problems that can affect particle data generated by LA-MC-ICP-MS include lag time differences between Faraday detectors and ion counters<sup>6,7</sup> and detector ‘blind time’, which affects the precision of isotopic data obtained using ultra short (<0.13 s) integration times.<sup>8</sup> Finally, instability in the ablation signal means data with near background-level ion beam intensities are common, and their highly anomalous isotope ratios can have a disproportionate effect on final isotopic compositions. For this reason, particle data cannot be processed using simple point-by-point averaging,<sup>6</sup> and alternative

<sup>a</sup>Lawrence Livermore National Laboratory, Livermore, CA 94550, USA. E-mail: wimpenny1@llnl.gov

<sup>b</sup>Savannah River National Laboratory, Aiken, SC 29808, USA

† Electronic supplementary information (ESI) available. See DOI: <https://doi.org/10.1039/d2ja00403h>



data reduction strategies are required to ensure accurate isotope ratios are produced with representative uncertainties. Thus, obtaining accurate and high-precision isotopic data for U particles is challenging not only from a technical standpoint, but also requires robust and reproducible data reduction procedures.

Several previous studies have developed methods to analyze U particles by laser ablation ICP-MS.<sup>6–15</sup> These studies have yielded U isotope ratios that are accurate within their stated precisions, with the caveat that data is highly imprecise in comparison to isotope ratios obtained by conventional solution analyses (<0.1%<sup>16</sup>). Here, we note that throughout this manuscript uncertainties are reported as two times the standard deviation of the mean, abbreviated as  $2\sigma$ . Typical published precision on the  $^{235}\text{U}/^{238}\text{U}$  ratios of U-particles measured by laser ablation ICP-MS range from 0.2 to 40% ( $2\sigma$ ), with higher precision data generated by multi-collector ICP-MS (over single collector instruments) and by ablating particles over 5  $\mu\text{m}$  in diameter.<sup>9–14</sup> For isotopic analyses of  $\leq 1\ \mu\text{m}$  diameter particles, which are most relevant to safeguards operations, precision of 1.8–6% ( $2\sigma$ ) has been achieved on the  $^{235}\text{U}/^{238}\text{U}$  ratio and 2.4–4.8% ( $2\sigma$ ) on the  $^{234}\text{U}/^{238}\text{U}$  ratio.<sup>7,15</sup> Although these results show that laser ablation is a promising technique for U particle analyses, several key aspects of technique development have remained untested. To date, most particle analyses have been performed on materials with natural or near-natural U isotopic compositions, meaning the capability to accurately analyze the isotopic composition of samples with higher than natural  $^{235}\text{U}$  enrichment levels have not been thoroughly assessed. Furthermore, because  $^{236}\text{U}$  does not exist in natural samples, the ability to characterize the  $^{236}\text{U}/^{238}\text{U}$  ratio has not yet been demonstrated, despite its importance to safeguards as a potential signature of reprocessing activity. Finally, correction factors for mass bias and ion counter gains have, up until now, been applied using pre-calculated constants that were derived from prior analyses of U reference materials in solution<sup>10</sup> or online aspiration of U standards prior to and after ablation.<sup>6</sup> Thus, shifts in these correction factors between and/or within each analytical session cannot be accounted for during particle analyses, potentially impacting the reproducibility of isotope ratio data.

Here, we aim to further develop LA-MC-ICP-MS as an analytical tool for safeguards evaluation by testing its performance during the isotopic analysis of two particulate reference standards; U.S. New Brunswick Laboratory Program Office (NBL PO) Certified Reference Material (CRM) U200, and DU-oxide particulates developed by SRNL. Both materials have well characterized and distinctive U isotopic compositions, with  $^{236}\text{U}$  contents that are resolvable above background.<sup>17,18</sup> In the case of SRNL-DU, its  $^{234}\text{U}$  and  $^{236}\text{U}$  contents are both extremely low (0.00068 and 0.0086% respectively), making it an ideal sample to assess the detection limits of LA-MC-ICP-MS with respect to LG-SIMS.<sup>18</sup> We also aim to streamline data collection by using an in-house U reference glass as a mass bias and ion counter gain standard, negating the need to pre-calibrate in solution mode or aspirate solutions into the plasma before and after each laser ablation analytical session. In theory, this approach

will also enable us to better account for in-run drift in mass bias, which may in turn help to improve the accuracy and precision of U isotopic data.

## 2. Experimental setup and methods

### 2.1. Hardware configuration

The analytical setup at Lawrence Livermore National Laboratory (LLNL) consists of a 193 nm excimer laser system with a 4 ns pulse length (Photon Machines Analyte), combined with a multi-collector—inductively coupled plasma—mass spectrometer (MC-ICP-MS, Thermo Scientific Neptune-Plus). The 193 nm laser energy is in the UV spectrum and couples well with IR transparent materials. Although the nanosecond pulse length is not as effective at reducing thermal effects of laser interaction with the sample surface as newer femtosecond laser systems, this is less important when ablating  $\mu\text{m}$ -scale particles, which are rapidly destroyed irrespective of the laser configuration. The Analyte laser ablation system is equipped with the two-volume 'Helex' laser cell, which ensures a rapid sample response rate and washout time and eliminates any spatial fractionation effects that occur within the sample chamber. Helium was supplied to the Helex cell and used as a carrier gas to transfer sample aerosol from the laser chamber to the ICP-MS. An additional argon gas was added to the carrier gas prior to sample introduction to the plasma. Testing was performed using a simple Tygon sample line from the chamber to the torch and comparing the performance with a sample homogenizing device (so called 'squid') to reduce spectral skew effects. No discernible difference in the accuracy or precision of isotope ratios was observed and, as such, all analyses were performed using the simple sample transfer line, which is less prone to accumulation of sample background.

The Neptune-Plus MC-ICP-MS at LLNL is equipped with 10 Faraday detectors, 3 full-size secondary electron multipliers (SEMs), and 3 compact discrete dynode detectors (CDDs). The ion counting configuration is designed for isotopic analyses of uranium, enabling intense ion beams of the major uranium isotopes ( $^{238}\text{U}$  and  $^{235}\text{U}$ ) to be measured on Faraday detectors and minor isotopes ( $^{233}\text{U}$ ,  $^{234}\text{U}$  and  $^{236}\text{U}$ ) to be measured using ion counters (Fig. S1†). Energy filters (or RPQs) on ion counter (IC)-1 and IC3 help to reduce scattering of ions and peak tailing that might affect accurate analysis of  $^{234}\text{U}$  and  $^{236}\text{U}$ . The  $^{235}\text{U}$  channel can be switched from Faraday to IC2 for low  $^{235}\text{U}$  materials, meaning that the detector configuration can be optimized for samples with varying  $^{235}\text{U}$  enrichment levels. The Neptune was fitted with high sensitivity cones ('Jet' sampler and 'X' skimmer) which increase sensitivity by  $\sim 3$  times over the standard ('H') cones. Faraday detectors were assigned with  $10^{11}\ \Omega$  resistors and Faraday preamplifier gain factors were measured prior to the start of each analytical session. Ion counter gain factors were calibrated during each session, as described in ESI-1.†

Samples were loaded into the laser ablation cell and the chamber was evacuated to remove air prior to filling with He carrier gas. After plasma ignition, the helium flow rates were set to  $\sim 0.6\ \text{l min}^{-1}$  in the Helex cell and  $\sim 0.5\ \text{l min}^{-1}$  in the internal



sampling cup. These flow rates and the argon sample gas were then optimized by tuning on the National Institute of Standards and Technology (NIST) 610 glass, which contains ~500 ppm U. Using a 50  $\mu\text{m}$  spot size, frequency of 7 Hz and fluence of  $2.1 \text{ J cm}^{-2}$ , a typical  $^{238}\text{U}$  intensity of 0.6–0.7 V was obtained, and instrument performance was evaluated at the start of each analytical session to ensure similar day-to-day performance. Typical instrument parameters used during LA-MC-ICP-MS analyses are provided in Table 1.

## 2.2. Samples and reference materials

**2.2.1. Reference glasses.** Several reference glasses were analyzed as part of this study to (i) determine optimal tuning parameters and day-to-day performance, (ii) assess the accuracy of isotope ratio measurements by laser ablation and (iii) calculate mass bias and ion counter gains factors. These reference materials included NIST 610, which has a relatively well characterized, depleted  $^{235}\text{U}/^{238}\text{U}$  ratio and low abundances of minor U isotopes (e.g. Duffin *et al.*<sup>23</sup>). Although a useful reference material for samples with near-natural U isotope ratios, NIST 610 is inappropriate for assessing the ability to measure samples with variably enriched isotopic compositions. It is also not ideal for determining instrumental mass bias due to the large disparity between  $^{235}\text{U}$  and  $^{238}\text{U}$  abundances. For this reason, a series of U-doped glasses prepared in house at LLNL from calcium–aluminum silicate base glasses were also used.<sup>19</sup> These materials range in  $^{235}\text{U}$  content from ~0.725% (natural U), ~50%, and ~93%, across two U concentrations (~50 and ~500 ppm). The isotopic compositions of these glasses were previously characterized by solution-mode MC-ICP-MS at LLNL<sup>19,20</sup> (Table S1†).

The wide range of reference material isotopic compositions enables robust evaluation of our ability to characterize samples with variable  $^{235}\text{U}$  enrichment levels and minor isotope abundances. To be of value for *in situ* isotopic analyses, either for QC purposes or as calibration standards, their spatial heterogeneity must be assessed. This was previously performed using secondary ionization mass spectrometry (NanoSIMS) at LLNL, and the Naval Ultra-Trace Isotope Laboratory's Universal Spectrometer (NAUTILUS), which is a SIMS—Single-Stage Accelerator Mass Spectrometry (SIMS-SSAMS)<sup>21</sup> at the U.S. Naval Research Laboratory.<sup>19</sup> The average composition of multiple *in*

*situ* analyses are presented in Table S2† and the degree of isotopic heterogeneity is represented by the reproducibility of the analyses (in-%). Based on these results, U-glass CAS-53-500 (~50%  $^{235}\text{U}$ , 500 ppm) has the most homogenous  $^{235}\text{U}/^{238}\text{U}$  composition, with relative uncertainties associated with duplicate  $^{235}\text{U}/^{238}\text{U}$  analyses of up to 0.4%. To further assess the suitability of CAS-53-500 as a mass bias standard for laser ablation analyses, we made 20 *in situ* isotopic analyses of U that were performed systematically over a 0.5 mm by 0.5 mm grid. During each isotopic analysis the  $^{238}\text{U}$  and  $^{235}\text{U}$  intensities were initially >100 mV, with internal precision on the raw  $^{235}\text{U}/^{238}\text{U}$  ratios of <0.03%. The external precision associated with the duplicate  $^{235}\text{U}/^{238}\text{U}$  analyses were <0.1%, including drift in the raw ratios caused by shift in instrumental mass bias. This indicates that any isotopic heterogeneities in the CAS-53-500 glass are well below the % level precision that is expected for isotopic analyses of U in  $\mu\text{m}$ -sized particles. Although a U-doped silicate glass is not a true matrix matched standard with  $\text{U}_3\text{O}_8$  particles, it can be assumed that slight discrepancies in mass bias between different analytes will be relatively inconsequential compared to the analytical uncertainty. Thus, given its subequal  $^{235}\text{U}$  and  $^{238}\text{U}$  abundances, well characterized minor isotope compositions, high U concentration (~500 ppm), and relatively homogenous isotopic composition, we infer that CAS-53-500 is the best available U standard to use for correction of mass bias and ion counter gain effects during U isotopic analyses by LA-MC-ICP-MS.

**2.2.2. Particle standards.** Two particle standards were prepared for this study. The first was an in-house particulate preparation of U.S. NBL PO CRM U200. This material was prepared for analysis by dispersing a slurry of U200 U-oxide powder ( $\text{U}_3\text{O}_8$ ) in ethanol onto a silicon planchet. The ethanol was allowed to evaporate and electrostatic forces kept the particles adhered to the silicon surface. Particle size distribution was not assessed for the U200 sample but based on observations using the optical microscope on the laser ablation system the grain sizes were mostly 2–5  $\mu\text{m}$ . The isotopic composition of U200 has been well characterized previously by multi-collector TIMS and is provided in Table S3.†<sup>16</sup> In addition to a  $^{235}\text{U}$  content of ~20%, U200 also contains relatively high  $^{234}\text{U}$  and  $^{236}\text{U}$  contents (0.1 and 0.2% respectively) that are easily resolvable from background levels. For example, if an individual U200 particle yielded a maximum  $^{238}\text{U}$  signal of ~100 mV, we would

Table 1 Basic instrumental parameters used during LA-MC-ICP-MS analyses

Neptune MC-ICP-MS		Photon machines analyte	
Sample cone	Jet	Helium 1 (main cell)	0.6 l min <sup>-1</sup>
Skimmer cone	X	Helium 2 (inner cup)	0.5 l min <sup>-1</sup>
Sample gas (Ar)	0.9–1.05 l min <sup>-1</sup>	Spot size ( $\mu\text{m}$ s)	40–85
Aux gas	0.8 l min <sup>-1</sup>	Ablation frequency	5–7 Hz
Cool gas	16 l min <sup>-1</sup>	Fluence ( $\text{J cm}^{-2}$ )	2.1–3.8
Center mass	254.15		
Integration time	0.13–0.26 s		
No. of integrations	200–400		
Resolution ( $m/\Delta m$ )	Low (400)		



expect minor isotope abundances of 0.1–0.2 mV, equating to 5–10 kcps on an ion counter. The second particle standard was  $\text{U}_3\text{O}_8$  with a highly depleted  $^{235}\text{U}$  content, which was produced by Savannah River National Laboratory (SRNL). This particle standard is referred to as SRNL-DU and its production process is described in detail by Scott *et al.* (2021).<sup>18</sup> In brief, an aerosol-based process was developed to monodisperse U particles with controllable particle size, phase and isotopic composition. The particles have well characterized size ( $\sim 1\ \mu\text{m}$ ) and density ( $\sim 8.3\ \text{g cm}^{-3}$ ) and a total of  $10^3$ – $10^5$  particles were deposited within a 10 mm diameter circle in the center of a silicon planchet. The U isotopic composition of SRNL-DU has been characterized previously by LG-SIMS<sup>18</sup> and is provided in Table S3.† As shown, the isotopic compositions of U200 and SRNL-DU differ significantly, and as such they are ideal test candidates to assess the capability of LA-MC-ICP-MS for characterizing the isotopic composition of U particles for safeguards purposes.

### 2.3. Analytical protocol

The basic architecture of each analytical sequence was the same, irrespective of whether glasses or particles were being analyzed. Each series of unknowns were bracketed by replicate analyses of the CAS-53-500 standard used to correct for instrumental mass bias and ion counter gains. Isotopic data was then

exported from the MC-ICP-MS in raw format and reduced using a bespoke data reduction code developed in R, an open-source statistical computing environment.<sup>22</sup> This workflow enables rapid, reliable and reproducible reduction of laser ablation data while incorporating relevant sources of uncertainty into the final ratio results. More details about data collection parameters for glasses and U particles are provided below.

**2.3.1. Glass analyses.** The data collection method for glass samples consisted of  $200 \times 0.26\ \text{s}$  integrations in static multi-collection mode, which equates to a total sampling time of  $\sim 50\ \text{s}$ . Although shorter integration times  $< 0.26\ \text{s}$  are possible using the Neptune, previous research has indicated that detector ‘blind time’ effects can reduce the proportion of signal that is detected and cause increased uncertainties on final isotope ratios.<sup>8</sup> Ablation of glasses was performed by ‘spot’ analyses, in which the laser is stationary and pulses down through the sample, producing the characteristic decaying signal with continued ablation (Fig. 1). An initial pre-ablation period was used to quantify the gas blank, or instrumental background, which was subtracted from the ablation signal. After  $\sim 20\ \text{s}$ , the laser is fired and point-by-point data is collected as the laser trace stabilizes, usually 2–5 s later, and continuing for  $\sim 30\ \text{s}$ . Although higher precision U isotope data can be obtained by performing line scans,<sup>23</sup> the transient data

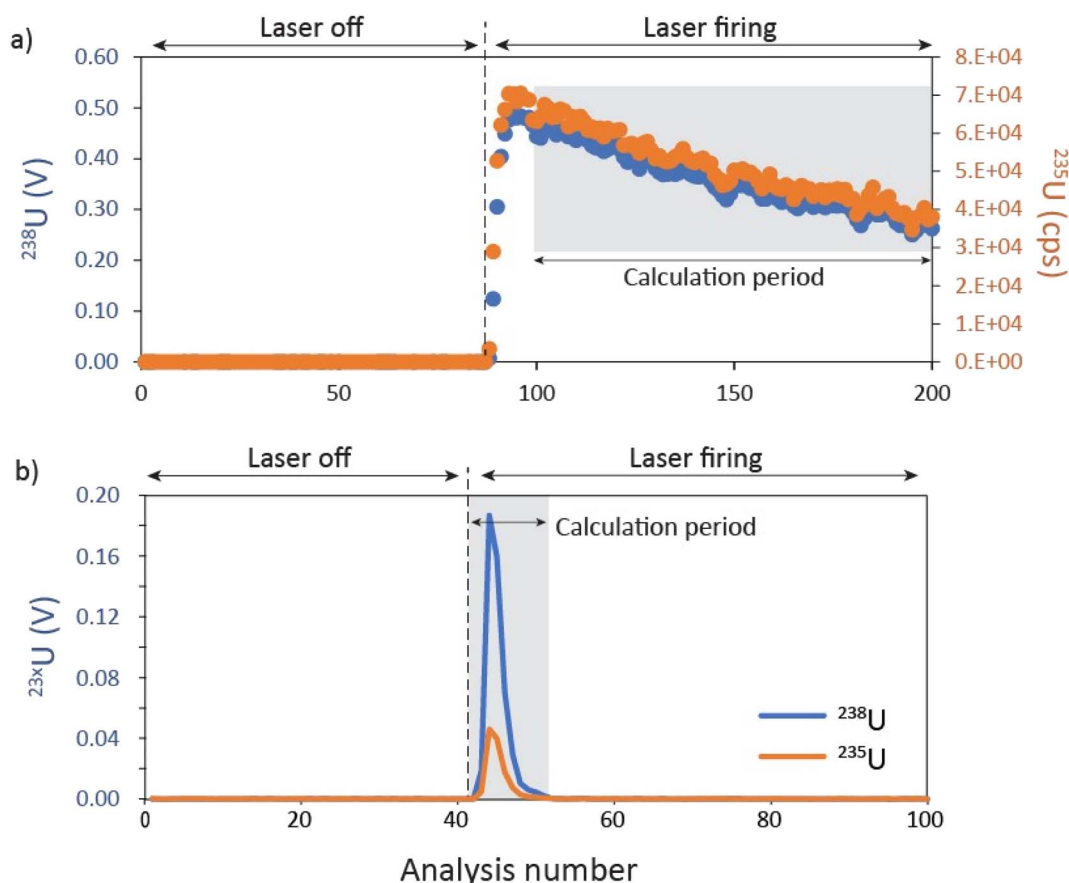


Fig. 1 Representative laser ablation traces derived from (a) pulsing down through a silicate glass (NIST-610), and (b) ablation of a single  $\mu\text{m}$ -scale particle of CRM U200.





generated by spot analyses are more representative of signals derived from a  $\mu\text{m}$ -scale particle.

**2.3.2. Particle analyses.** The primary difference between ablation of glasses and  $\mu\text{m}$  sized U-particles is the speed at which the U particles are ablated and the ephemeral nature of the resulting U signal. Complete ablation/consumption of a  $\mu\text{m}$ -scale particle takes place within  $\sim 3$  pulses, and complete ablation is achieved irrespective of the laser fluence in the range tested. Particle ablation can be performed manually or through an automated rastering process. For manual ablation, individual samples were pre-identified on the sample planchet using the laser ablation optics, and blocks of 6–8 particles were bracketed by analyses of the CAS-53-500 standard for time-resolved correction of mass bias and ion counter gains. Each particle analysis consisted of  $100 \times 0.26$  s integrations. A 10 s pre-ablation period was followed by ablation of each particle, in which  $\sim 2$  s of U data was generated. However, a major drawback of manually identifying  $\mu\text{m}$  sized U particles is that they are at the limit of what can be resolved using an optical microscope, meaning the process is slow and, in some cases, inaccurate. It is possible to misidentify U particles for unknown ‘others’ such as dust particles or imperfections in the silicon planchet surface. Due to this lack of efficiency a rastering method was established, wherein an area of 0.5–1.0  $\text{mm}^2$  was preselected on the silicon planchet and the laser was rastered across the area in a grid pattern with spot size of 25  $\mu\text{m}$  and a constant laser ‘dose’ that was imparted to each spot. In this case, the dose rate was 3 pulses per spot and, as the frequency was kept at 3 Hz, each spot was ablated for 1 s before the laser moved on. To collect the data generated from a large area raster requires a prolonged analytical method to be setup on the mass spectrometer. In this case, the Neptune’s method editor was configured for a single block of 0.26 s integrations, equating to a total sampling time of 30–60 min. Concerns about mixing between signals generated by one or more neighboring particles are valid during a rastering procedure, particularly in situations where particles with heterogeneous isotopic compositions are present. With our current laser ablation cell, signal from a single particle is detected for 2–4 s (Fig. S2†), hence mixing of signals generated by closely packed U particles could occur. In future studies this effect could be rectified by longer ablating at each spot (e.g. 9–12 pulses or 3–4 s), giving the U signal time to decay down to background levels after the particle is ablated away. However, the added time required to establish the complete washout of signal to background levels would effectively quadruple the time taken to ablate a given area, which would have negative consequences for rastering efficiency and sample throughput. It should be recognized that  $\sim 90\%$  of the total U signal from a single particle is detected within 1 s of ablation, and 99% detected within 2 s using the current setup (Fig. S2†). Thus, a sampling time of  $\sim 2$  s per spot could be an optimal compromise to ensure relatively rapid analysis of particles deposited over large areas, while also minimizing cross-talk and mixing between aerosols derived from neighboring particles. Alternatively, different methods and/or hardware modifications to

decrease sample washout time would be required to prevent signal mixing.

## 2.4. Data reduction

Reduction of U isotopic data from the ablation of silicate glasses and  $\text{U}_3\text{O}_8$  particles follow similar basic principles, requiring characterization of instrument backgrounds, isolation of raw data for each sample and standard, followed by application of correction factors for average blank, instrumental mass bias and ion counter gain. Solution based MC-ICP-MS analyses of U also apply additional corrections for peak tailing (i.e. the half-mass baseline), and U-hydride interference on  $^{236}\text{U}$ . However, given the relatively low precision of U isotopic analyses by laser ablation (i.e. %-level on  $^{236}\text{U}/^{238}\text{U}$ ), it is likely that any such corrections have negligible effect on the final isotope ratios. Moreover, it is not practical to perform an on-peak half mass baseline correction for *in situ* analyses that produce highly transient ion beams.

For glass samples, isolation of the raw data and calculation of raw isotope ratios are relatively straightforward; after  $\sim 5$  s stabilization period the point-by-point U isotope data is simply averaged and the uncertainty is calculated as the standard error of the mean. Although U intensities decay during spot analyses, there is no accompanying drift in the U isotope ratios, consistent with the fact that simultaneous detection of ion beams overcomes the relatively stable changes in intensity generated by ablating down through a sample. Typical precision on the raw  $^{235}\text{U}/^{238}\text{U}$  ratio generated from a single spot analysis on CAS-53-500 was 0.03–0.05% ( $2\sigma$ ).

As described in Section 1, accurate and representative reduction of U particle data must overcome detrimental effects such as time lag differences between detectors and skewing of final isotopic data by anomalous low-level data points. Thus, simple averaging of point-by-point isotopic data produces final isotope ratios that are highly imprecise. Several methods have been used to overcome these challenges, including integrating the total signal for a given sample,<sup>14</sup> synchronizing signals by using a linear regression slope<sup>6,7,14</sup> and development of a finite mixture model.<sup>7</sup> Despiking routines have also been developed to exclude data points with highly anomalous isotopic compositions.<sup>14</sup> Here, we used the integration method to reduce U isotope data from individual particles. This is a relatively simple reduction method that effectively gives more weighting to data points with higher  $^{238}\text{U}$  intensities, while also taking background intensities into account. Based on the scatter in the background prior to and after the sample signal we established a threshold value of 0.3 mV of  $^{238}\text{U}$ , above which we assume we are recording the U isotope signal associated with the particle rather than fluctuations in the background. Final uranium data was integrated for all data points with  $^{238}\text{U}$  intensity  $>0.3$  mV. Uncertainties associated with these summed counts were estimated based on counting statistics. Typical uncertainties on  $^{235}\text{U}/^{238}\text{U}$  for a single particle of U200 are 3–4 times lower than using the point-by-point reduction method. The procedures required to reduce U-particle data by the integration method



and the assignment of representative internal uncertainties are detailed below:

- Sample intensities/voltages are summed over the data collection period where  $^{238}\text{U} > 0.3$  mV (Fig. 1b).
- Integrated Faraday signals for  $^{238}\text{U}$  and  $^{235}\text{U}$  are converted into intensities (cps) assuming that 1 mV = 62 415 counts per second (cps).
- Uncertainties associated with the integrated sample signal are calculated as follows:

$$\text{Std. Uncert. } ^{23x}\text{U}_{\text{sample}} = \sqrt{\sum ^{23x}\text{U}_{\text{sample}}} \quad (1)$$

where  $\sum ^{23x}\text{U}_{\text{sample}}$  refers to the number of counts of isotope  $^{23x}\text{U}$  from each particle (shaded region, Fig. 1b), where  $x$  represents  $^{234}\text{U}$ ,  $^{235}\text{U}$ ,  $^{236}\text{U}$  or  $^{238}\text{U}$ .

However, eqn (1) underestimates uncertainty in practice, because it does not take into account noise from the detector. This consideration is particularly important for isotopes measured by Faraday detector as mV signals equate to count rates of 10's–100's k cps, which generate very low uncertainties based solely on counting statistical assumptions. Because mV-level signals are close to background levels on the Faraday detectors, any instability in that background signal adds a significant additional uncertainty to the final sample analysis and must be explicitly incorporated. To this end, total  $^{23x}\text{U}$  background counts for each isotope are calculated using eqn (2), where  $\sigma^{23x}\text{U}$  is the standard deviation of the background for isotope  $^{23x}\text{U}$  (in cps), and  $N^{23x}\text{U}_{\text{sample}}$  is the number of data points that are integrated for each sample.

$$\sum ^{23x}\text{U} = \sigma^{23x}\text{U}_{\text{background}} \times N^{23x}\text{U}_{\text{sample}} \quad (2)$$

- The sample and background uncertainties are then summed to obtain a final measurement uncertainty for each isotope:

$$\text{Std. Uncert. } ^{23x}\text{U}_{\text{Total}} = \text{Std. Uncert. } ^{23x}\text{U}_{\text{sample}} + \sum ^{23x}\text{U} \quad (3)$$

- The final uncertainties for each ratio are then calculated using eqn (4):

$$\text{Std. Uncert. } \left( \frac{^{23x}\text{U}}{^{238}\text{U}} \right) = \frac{\sum ^{23x}\text{U}}{\sum ^{238}\text{U}} \times \sqrt{\left( \frac{\text{Std. Uncert. } ^{23x}\text{U}_{\text{Total}}}{\sum ^{23x}\text{U}} \right)^2 + \left( \frac{\text{Std. Uncert. } ^{238}\text{U}_{\text{Total}}}{\sum ^{238}\text{U}} \right)^2} \quad (4)$$

Once raw data and associated uncertainties are obtained for glass and/or particle samples, those data must be corrected for mass bias effects and differences in ion counter performance (*i.e.* the ion counter gain). These correction factors are not constants, but rather change both between and within individual analytical sessions, which must be accounted for during setup of the analytical routine and during data processing. Detailed description of how these correction factors were calculated are provided in ESI-1.†

Due to the large amount of data generated by laser ablation analyses and the complexity involved with accurate correction of the data, an automated data reduction script was written in the statistical programming language *R*<sup>22</sup>. This approach ensured a robust and consistent treatment of U isotopic data and associated uncertainties for all samples and standards.

### 3. Results and discussion

#### 3.1. Isotopic analyses of U in silicate glasses by LA-MC-ICP-MS

Summarized results of the isotopic analyses of NIST-610 and the three U-doped glass standards are provided in Table 2, with corrected ratios provided in Table S4† and plotted in Fig. S3 and S4.†

**3.1.1. NIST-610.** Isotopic analyses of NIST-610 highlight that the chemical composition of the sample matrix and isotopic composition of U play an important role in governing data quality. Thus, although  $^{235}\text{U}/^{238}\text{U}$  ratios were accurate to within 1.7%, the average  $^{234}\text{U}/^{238}\text{U}$  and  $^{236}\text{U}/^{238}\text{U}$  ratios were 13 and 3.3% higher than reference values.<sup>23,24</sup> This contrasts with the results of Duffin *et al.* (2015),<sup>23</sup> who obtained accurate and highly precise  $^{234}\text{U}/^{238}\text{U}$  and  $^{236}\text{U}/^{238}\text{U}$  data for NIST-610 using femto-second LA-MC-ICP-MS. This discrepancy between the two studies is likely to stem from differences in analytical protocol. First, Duffin *et al.* (2015) performed line scans on the surface of the glass, rather than spot analyses. This produces a higher and more stable ion beam that reduces uncertainties associated with the raw ratio measurement. Second, and perhaps more importantly, Duffin *et al.* (2015) performed their analyses in medium- and high-resolution modes ( $m/\Delta m = 4000$  and 10 000), which allowed polyatomic interferences to be resolved from the various isotopes of uranium. NIST-610 is well known to have an elevated Pt content due to its preparation in a Pt-Rh lined furnace<sup>24</sup> and the polyatomic species  $^{194}\text{Pt}^{40}\text{Ar}^+$  and  $^{196}\text{Pt}^{40}\text{Ar}^+$  would be difficult to resolve from  $^{234}\text{U}$  and  $^{236}\text{U}$  at low resolution. Although the Neptune-plus at LLNL is capable of

**Table 2** Average U isotope ratios measured in NIST 610 and three in-house U reference glasses by LA-MC-ICP-MS. Uncertainties are external precisions associated with replicate analyses at the 2σ level ( $n = 15$ ). Offset proportions are relative to the reference values presented in Table 2

	$^{234}\text{U}/^{238}\text{U}$	2σ	RSD (%)	Offset (%)	$^{235}\text{U}/^{238}\text{U}$	2σ	RSD (%)	Offset (%)	$^{236}\text{U}/^{238}\text{U}$	2σ	RSD (%)	Offset (%)
NIST 610	0.0000107	0.0000004	3.51	13.4	0.0023544	0.0000032	0.14	−1.7	0.0000445	0.0000005	1.20	3.3
CAS3-94-500	0.1701	0.0010	0.60	1.1	16.101	0.025	0.16	1.2	0.05090	0.00041	0.81	1.2
SAC-53-50	0.007823	0.000037	0.48	0.2	1.1004	0.0015	0.14	0.2	0.005518	0.000035	0.64	0.4
SAC-53-500	0.007995	0.000042	0.53	−0.3	1.12601	0.00039	0.03	−0.2	0.005652	0.000034	0.61	0.1



performing isotopic analyses at high resolving power, this reduces the transfer of ions through the mass spectrometer by up to a factor of 10, which is problematic given the sample-limited nature of particle analyses. Because NIST 610 has only trace amounts of  $^{234}\text{U}$  and  $^{236}\text{U}$  (isotopic abundances of <50 ppm) and uniformly high trace element concentrations (400–500 ppm), the minor U isotope ratios are far more susceptible to interferences generated by polyatomic species than either the in-house glass standards or U-oxide particles. New generations of MC-ICP-MS are utilizing collision cell technology to remove potential interferences and matrix elements online, which could help to improve laser ablation capabilities in the future for samples with complex matrices.

**3.1.2. LLNL U-doped glasses.** In contrast to NIST-610, the average  $^{234}\text{U}/^{238}\text{U}$ ,  $^{235}\text{U}/^{238}\text{U}$  and  $^{236}\text{U}/^{238}\text{U}$  ratios of the SAC-53-50 and SAC-53-500 glasses fell within 0.4% of reference values, with standard deviations of the replicate analyses ranging from 0.03 to 0.6%. Replicate  $^{235}\text{U}/^{238}\text{U}$  ratios were more reproducible (0.03–0.14%) than  $^{234}\text{U}/^{238}\text{U}$  and  $^{236}\text{U}/^{238}\text{U}$  ratios (0.48–0.64%), which is expected given that both  $^{235}\text{U}$  and  $^{238}\text{U}$  were measured on Faraday detectors. Although SAC-53-500 contains ~10 times more U than SAC-53-50, there was no significant difference in data quality between the two materials. The glass with the highest  $^{235}\text{U}$  enrichment, CAS-94-500, yielded  $^{234}\text{U}/^{238}\text{U}$ ,  $^{235}\text{U}/^{238}\text{U}$  and  $^{236}\text{U}/^{238}\text{U}$  ratios that were systematically ~1.2% higher than the reference values. This is significant, given that the standard deviation of replicate analyses ranged from 0.16 to 0.8%. To understand the cause of these offsets, we plotted

$^{235}\text{U}/^{238}\text{U}$  vs.  $^{234}\text{U}/^{238}\text{U}$  for the laser ablation and solution MC-ICP-MS analyses (Fig. S5†). As shown, the solution data form a well constrained mixing line between a highly  $^{235}\text{U}$  enriched endmember and low  $^{235}\text{U}$  enriched contaminant, with the laser ablation data lying in a cluster at the highly enriched end. We hypothesize that the CAS-94-500 sample aliquots that were prepared for solution mode analysis were variably contaminated by U with a near natural isotopic composition. Given the extreme difference in isotopic composition between U in the sample (>90%  $^{235}\text{U}$ ) and natural U (~0.007%  $^{235}\text{U}$ ), even a small amount of contaminant addition to the sample would significantly affect the isotopic composition of U. Because laser ablation samples are not processed through chemistry, and so not affected by contaminant addition, the derived U isotope data are likely to be more accurate. This illustrates one of the major benefits of U isotopic analysis by laser ablation; there is no addition of U blank during sample handling/processing that could potentially alter the final U isotope ratio.

**3.1.3. Uncertainty budgets.** For the four glass samples, combined standard uncertainties (CSU) on individual  $^{235}\text{U}/^{238}\text{U}$  ratios were between 0.25 and 0.7% ( $2\sigma$ ), whereas CSU's on  $^{234}\text{U}/^{238}\text{U}$  and  $^{236}\text{U}/^{238}\text{U}$  ratios ranged from 0.5–2.5%. These uncertainties are a similar order of magnitude to the external precision ( $2\sigma$ ), calculated from the standard deviation of each sample population (Table 2). This observation indicates that the calculation of uncertainties for individual particles is robust. Typical uncertainty budgets for the  $^{235}\text{U}/^{238}\text{U}$  and  $^{234}\text{U}/^{238}\text{U}$  ratios measured during isotopic analyses of the glasses are

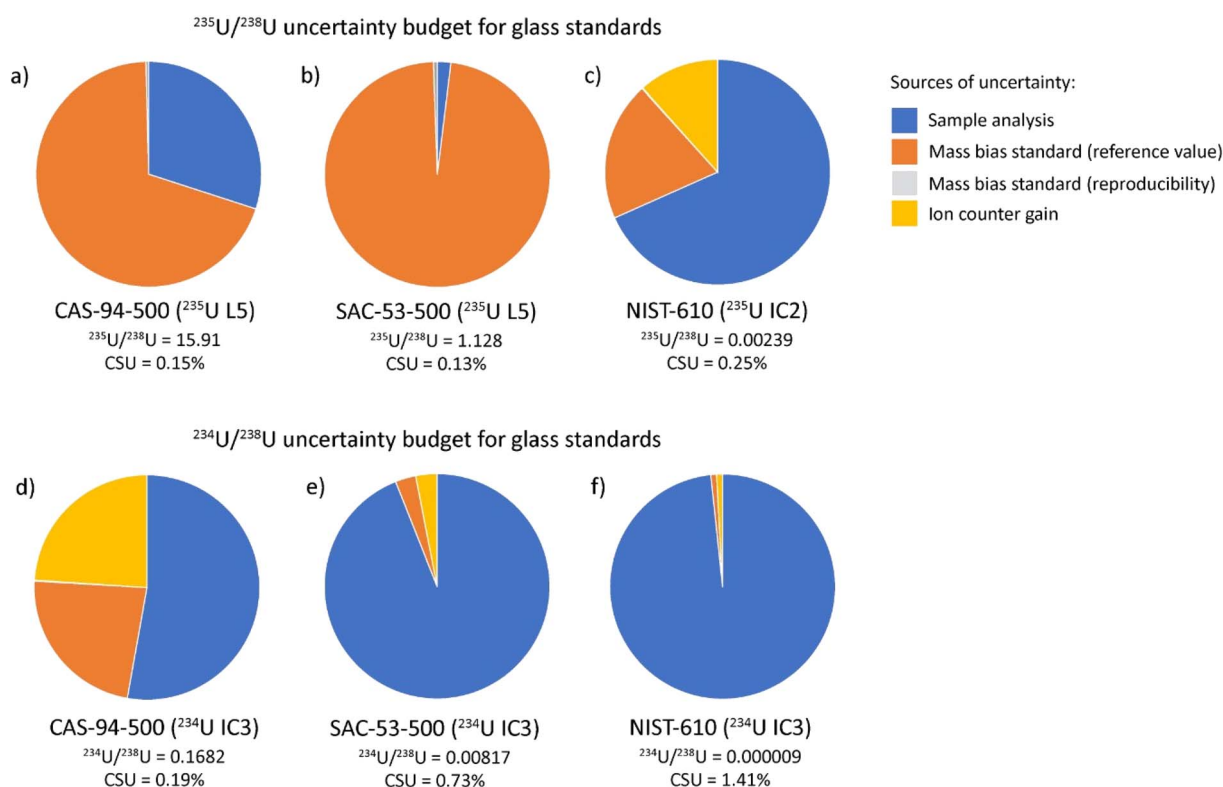


Fig. 2 Uranium isotope ratio uncertainty budgets for the three glass standards. The uncertainty budgets for  $^{235}\text{U}/^{238}\text{U}$  are provided in (a–c) and uncertainty budgets for  $^{234}\text{U}/^{238}\text{U}$  are provided in (d–f).



presented in Fig. 2. Here, the uncertainty budget for  $^{234}\text{U}/^{238}\text{U}$  serves as an analog for  $^{236}\text{U}/^{238}\text{U}$  because  $^{234}\text{U}$  and  $^{236}\text{U}$  were both analyzed using ion counters and had similar count rates. The major sources of uncertainty for each individual isotopic measurement are: (i) the blank corrected ratios, (ii) the known isotopic composition of the mass bias standard, (iii) reproducibility of the mass bias standard measurement and, where ratios are measured by ion counter, (iv) the uncertainty associated with the ion counter gain correction. The uncertainty of the mass bias standard is a critical parameter as it constrains the minimum uncertainty that can be achieved for any sample, either glass or particle. Thus, as the uncertainty associated with the reference  $^{235}\text{U}/^{238}\text{U}$  ratio of CAS-53-500 is 0.13%, precision better than this value cannot currently be attained for U isotope ratios of unknowns.

As shown in Fig. 2a–c, the uncertainty budget for  $^{235}\text{U}/^{238}\text{U}$  is highly dependent on the isotopic composition of U in the glass. For SAC-53-500, there are subequal amounts of  $^{235}\text{U}$  and  $^{238}\text{U}$ , meaning voltages produced for both isotopes are relatively high (>100 mV) and the error associated with the sample measurement is ~2% of the final uncertainty. Instead, the uncertainty of the isotopic composition of the mass bias standard accounts for ~98% of the error. This indicates that changes in data collection or experimental parameters would not greatly improve the final CSU of the isotopic analyses. The analytical uncertainty associated with the raw ratios becomes more important where there is greater disparity in the contents of  $^{235}\text{U}$  and  $^{238}\text{U}$ , accounting for ~30% of the total uncertainty in CAS-94-500. For NIST-610, the  $^{235}\text{U}$  signal is measured by ion counter and the sample measurement contributes the dominant source of uncertainty (~70%).

The uncertainty budget for the minor isotope ratios ( $^{234}\text{U}/^{238}\text{U}$  and  $^{236}\text{U}/^{238}\text{U}$ ) are dominated by uncertainty associated with the sample analysis, which accounts for >50% of total uncertainty for the four glass samples (Fig. 2d–f). In detail, our analyses show that glasses with higher minor isotope abundances give higher precision  $^{234}\text{U}/^{238}\text{U}$  and  $^{236}\text{U}/^{238}\text{U}$  ratios, as is expected given that higher  $^{234}\text{U}$  and  $^{236}\text{U}$  contents generate higher count rates. Thus, the sample with the highest  $^{234}\text{U}$  and  $^{236}\text{U}$  contents (CAS-94-500) has the lowest fraction of the total uncertainty budget from the sample analysis.

### 3.2. U-particle analyses

**3.2.1. CRM U200.** A total of 49 particles of CRM U200 were analyzed as part of this study, with the results summarized in Table 3 and presented in Fig. 3, and the full data set provided in Table S5.† Particles of U200 varied in size and, based on

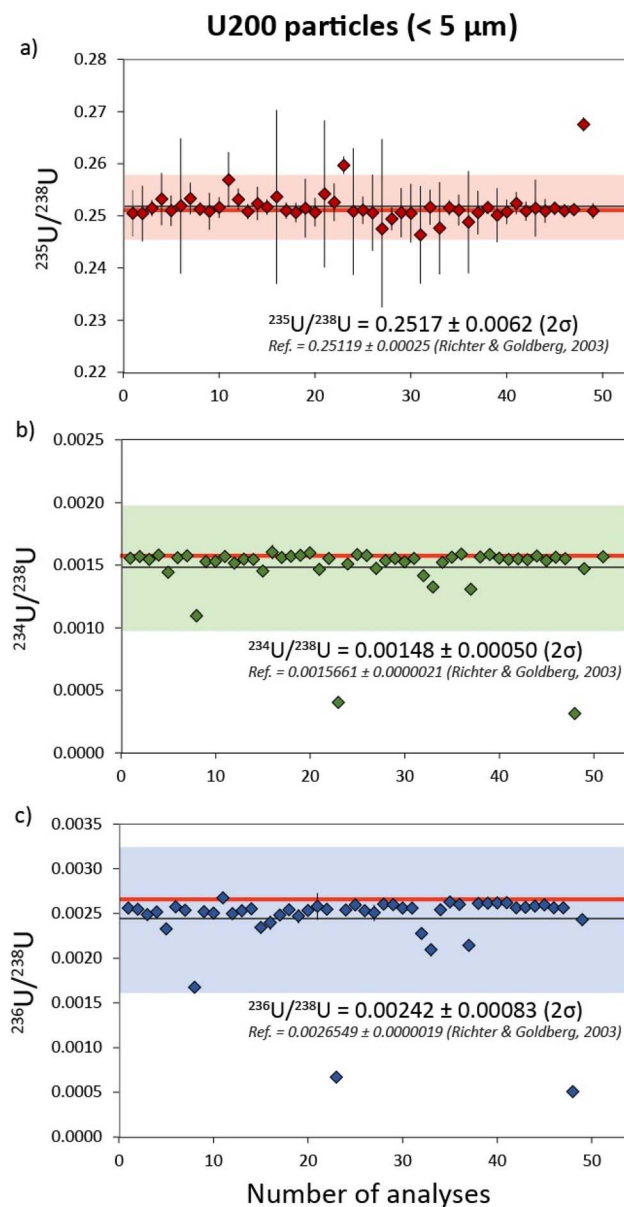


Fig. 3 Uranium isotope systematics for 49 separate U200 particles with  $^{235}\text{U}/^{238}\text{U}$ ,  $^{234}\text{U}/^{238}\text{U}$  and  $^{236}\text{U}/^{238}\text{U}$  data in (a), (b) and (c) respectively. Reference isotope ratios (red) are taken from Richter & Goldberg.<sup>16</sup> Uncertainties are 2σ.

observations using the laser ablation optics, were between <1 and 5 μm in diameter, equating to total U masses between 4 and 400 pg. Typical  $^{238}\text{U}$  and  $^{235}\text{U}$  intensities from the ablation of a single particle ranged from 10 s to 100 s of mV and generated

**Table 3** Uranium isotope data from replicate analyses of the U200 particles. Uncertainties are external precisions associated with replicate analyses at the 2σ level. Data is provided with and without outlier rejection for the  $^{234}\text{U}/^{238}\text{U}$  and  $^{236}\text{U}/^{238}\text{U}$  ratios

	$^{234}\text{U}/^{238}\text{U}$	2σ	RSD (%)	$^{235}\text{U}/^{238}\text{U}$	2σ	RSD (%)	$^{236}\text{U}/^{238}\text{U}$	2σ	RSD (%)
All data (n = 49)	0.00148	0.00050	34.0	0.2517	0.0062	2.5	0.00242	0.00083	34.3
Outliers excluded (n = 40)	0.001549	0.000031	2.0	N/A	N/A	N/A	0.00255	0.00010	3.8
Reference value <sup>16</sup>	0.0015661	0.0000021	0.1	0.25119	0.00025	0.1	0.0026549	0.0000019	0.1





2–4 s of data. Because  $^{235}\text{U}$  constitutes  $\sim 20\%$  of the total U in U200, both  $^{235}\text{U}$  and  $^{238}\text{U}$  were analyzed using Faraday detectors, whereas  $^{234}\text{U}$  and  $^{236}\text{U}$  were analyzed using ion counters. The average  $^{235}\text{U}/^{238}\text{U}$  ratio of the 49 U200 particles was  $0.2517 \pm 0.0062$  ( $2\sigma$ ), which is within uncertainty of the reference value<sup>16</sup> (see Table S3†). The standard deviation of the 49  $^{235}\text{U}/^{238}\text{U}$  ratios equates to an external precision of  $\sim 2.5\%$  ( $2\sigma$ ), which is of a similar magnitude to the CSU of  $^{235}\text{U}/^{238}\text{U}$  ratios in individual particles (see Section 3.2.3. for further discussion of uncertainty budget). As expected from such a transient, highly unstable signal, the  $^{235}\text{U}/^{238}\text{U}$  data are an order of magnitude more heterogeneous than data generated by the U reference glasses (relative standard deviation [RSD]'s of 0.03–0.14%, Section 3.1). However, the standard deviation of the  $^{235}\text{U}/^{238}\text{U}$  ratios is similar to those previously obtained by LA-MC-ICP-MS analyses of  $\mu\text{m}$  scale U-particles ( $1.8\text{--}6\%^{7,8}$ ).

In contrast to  $^{235}\text{U}/^{238}\text{U}$ , the measured minor U isotope ratios ( $^{234}\text{U}/^{238}\text{U}$  and  $^{236}\text{U}/^{238}\text{U}$ ) exhibited a greater degree of scatter, equating to RSDs ( $2\sigma$ ) of  $\sim 34\%$ . However, much of this apparent variability was generated by a subset of U200 particles with  $^{234}\text{U}/^{238}\text{U}$  ratios that covary with  $^{236}\text{U}/^{238}\text{U}$  and fall outside of uncertainty from the main sample population (Fig. 4). This

indicates that the U200 material was mixed with a contaminant that was relatively depleted in  $^{234}\text{U}$  and  $^{236}\text{U}$  contents (Fig. 4a) and, to a lesser extent, relatively enriched in  $^{235}\text{U}$  (Fig. 4b). If the particles that fall on this correlation line are excluded, the reproducibility of  $^{234}\text{U}/^{238}\text{U}$  and  $^{236}\text{U}/^{238}\text{U}$  values in the remaining populations are improved to 2 and 3.8% respectively (Table 3). The origin of this contaminant phase cannot currently be ascertained. In theory, it may be inherent to the U200 reference material or was added during sample preparation at LLNL. The two-component mixing array is likely to reflect variable agglomeration of particles with these two isotopically distinct U compositions. At the bulk level, this contaminant phase is unlikely to be significant as it only imparts minor variations to the U isotope ratios and the heterogeneities are only observed in a subset of U particles ( $\sim 20\%$ ). However, this neatly illustrates the effectiveness of characterizing U-isotope ratios at the particle scale by laser ablation MC-ICP-MS and the potential for identifying isotopic signatures that may not be apparent using bulk dissolution techniques.

**3.2.2. Depleted uranium particles (SRNL-DU).** The DU particles obtained from SRNL are composed of  $\text{U}_3\text{O}_8$  that was produced purposely for *in situ* isotopic analyses. A total of 103

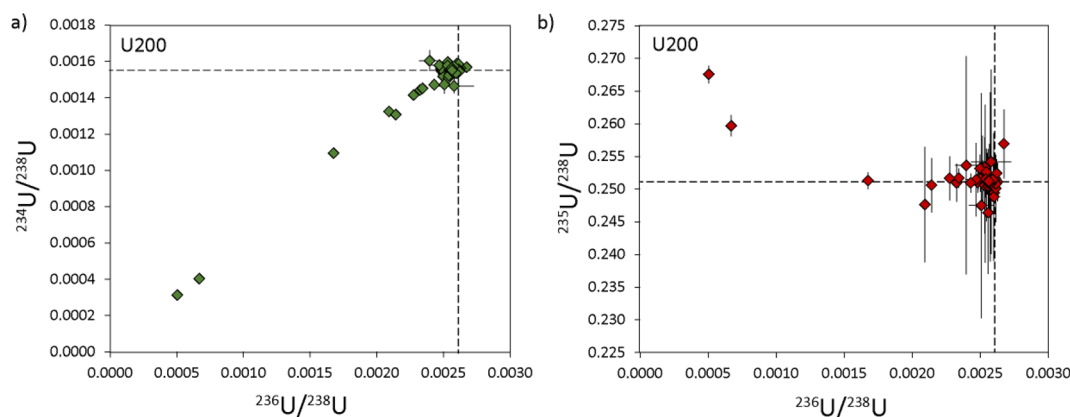


Fig. 4 Three isotope plots of the uranium composition in U200 particles with  $^{234}\text{U}/^{238}\text{U}$  vs.  $^{236}\text{U}/^{238}\text{U}$  in (a) and  $^{235}\text{U}/^{238}\text{U}$  vs.  $^{236}\text{U}/^{238}\text{U}$  in (b). Reference values (dashed lines) are from Richter & Goldberg.<sup>16</sup> All uncertainties are  $2\sigma$ .

**Table 4** Uranium isotope data for the SRNL-DU particle sample obtained by laser ablation. Data for  $^{234}\text{U}/^{238}\text{U}$  and  $^{236}\text{U}/^{238}\text{U}$  derive from 103 separate analyses. Data for  $^{235}\text{U}/^{238}\text{U}$  with  $^{235}\text{U}$  on IC2 derive from 36 measurements, whereas data with  $^{235}\text{U}$  on L5 derive from 62 measurements. Uncertainties are external precision associated with replicate analyses at the  $2\sigma$  level

Isotopic composition	$^{234}\text{U}/^{238}\text{U}$	$2\sigma$	$^{235}\text{U}/^{238}\text{U}$	$2\sigma$	$^{236}\text{U}/^{238}\text{U}$	$2\sigma$
Laser ablation ( $^{235}\text{U}$ IC2)	0.0000071	0.0000025	0.001677	0.000030	0.000078	0.000014
Laser ablation ( $^{235}\text{U}$ L5)			0.0016	0.0013		
LG-SIMS (single particle) <sup>a</sup>	0.0000068	0.0000035	0.00173	0.00010	0.0000807	0.0000086
LG-SIMS (particle mapping) <sup>a</sup>	0.0000088		0.00174		0.000079	
Isotopic distribution	$^{234}\text{U}$	$^{235}\text{U}$	$^{235}\text{U}$	$^{235}\text{U}$		
Laser ablation (LLNL)	0.00071%	0.1674%	0.0078%	99.82%		
LG-SIMS <sup>a</sup>	0.00068%	0.1720%	0.00804%	99.640%		

<sup>a</sup> Reference values from LG-SIMS analyses are from Scott *et al.*<sup>18</sup>.



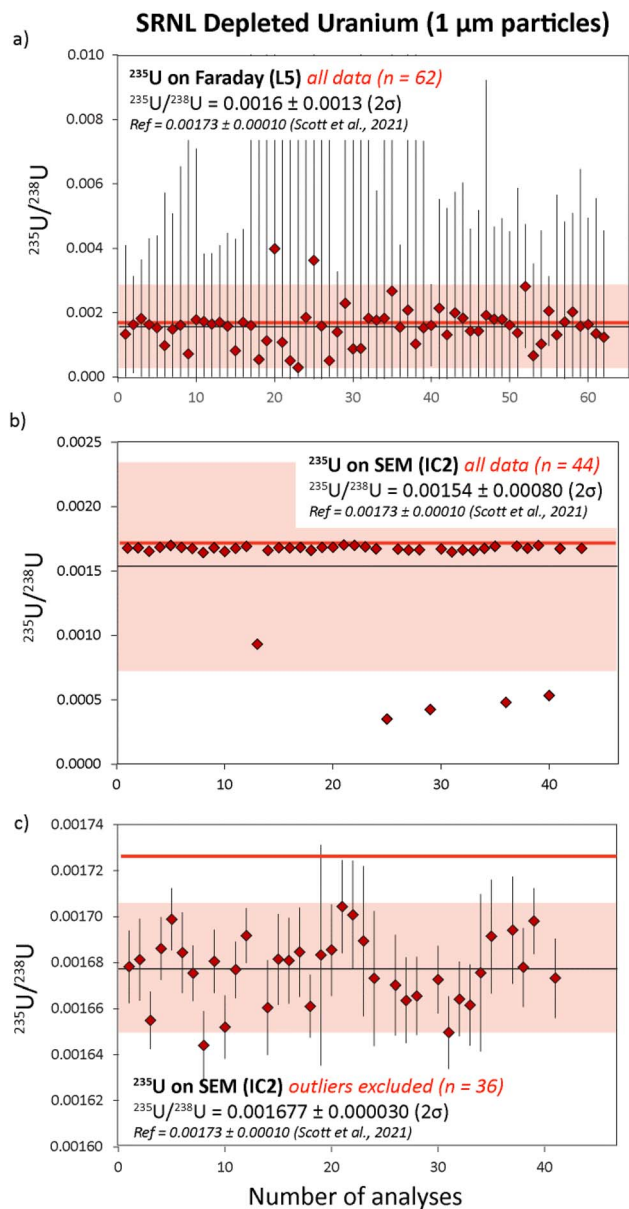


Fig. 5  $^{235}\text{U}/^{238}\text{U}$  ratios measured in SRNL-DU particles. In (a) the  $^{235}\text{U}$  was analyzed using the L5 Faraday. In (b) the  $^{235}\text{U}$  content was measured using IC2, and the final  $^{235}\text{U}/^{238}\text{U}$  average with five outliers excluded are in (c). Reference isotope ratios (red) are taken from Scott et al.<sup>18</sup> All uncertainties are  $2\sigma$ .

SRNL-DU particles were analyzed for this study, with a roughly even split between those analyzed with  $^{235}\text{U}$  on the L5 Faraday and those analyzed with  $^{235}\text{U}$  on IC2. The results of these analyses are summarized in Table 4 and displayed in Fig. 5 and 6, with the full dataset provided in Table S6.<sup>†</sup>

The SRNL-DU sample has a  $^{235}\text{U}$  content of  $0.1720 \pm 0.0104\%$ , meaning the  $^{235}\text{U}$  content is highly depleted compared to either natural U or U200. Maximum  $^{235}\text{U}$  signals on the L5 Faraday were 3–4 mV, which is difficult to resolve from the background noise on the detector. Consequently, the  $^{235}\text{U}/^{238}\text{U}$  ratios obtained with  $^{235}\text{U}$  on the L5 Faraday were highly dispersed, with an average ratio of  $0.0016 \pm 0.0013$  ( $2\sigma$ )

from 62 measurements (Fig. 5a). After  $2\sigma$  outlier rejection, the statistics were improved slightly to  $0.0015 \pm 0.0010$  ( $2\sigma$ ) from 60 measurements. This equates to an RSD of 67%, a value that is broadly consistent with internal CSU values that range between 50–200%. Although the Faraday–Faraday  $^{235}\text{U}/^{238}\text{U}$  data are highly imprecise, we note that they are within uncertainty of the reference value for SRNL-DU. As would be expected, the  $^{235}\text{U}/^{238}\text{U}$  ratios generated with  $^{235}\text{U}$  on IC2 were far more precise. In this case, typical  $^{235}\text{U}$  counts on IC2 were  $\sim 10$ – $12$  k cps, which were easily measurable above background levels ( $< 5$  cps). If all data were included, we obtained a final average  $^{235}\text{U}/^{238}\text{U}$  ratio of  $0.00154 \pm 0.00080$  ( $2\sigma$ ), as shown in Fig. 5b.

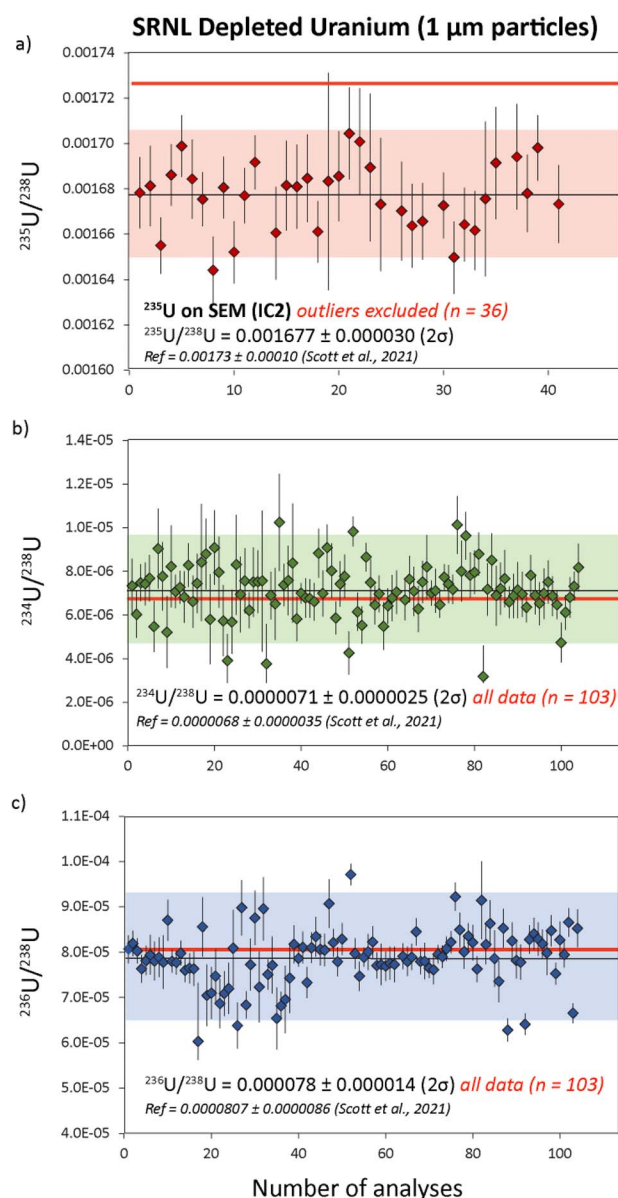


Fig. 6 Uranium isotope data from replicate analyses of SRNL-DU particles with  $^{235}\text{U}/^{238}\text{U}$ ,  $^{234}\text{U}/^{238}\text{U}$  and  $^{236}\text{U}/^{238}\text{U}$  data in (a), (b) and (c) respectively. Five outliers were rejected from the  $^{235}\text{U}/^{238}\text{U}$  population based on  $2\sigma$  of the mean. Samples with outlying  $^{235}\text{U}/^{238}\text{U}$  ratios did not have outlying  $^{234}\text{U}/^{238}\text{U}$  and  $^{236}\text{U}/^{238}\text{U}$  ratios. Reference isotope ratios (red) are taken from Scott et al.<sup>18</sup> All uncertainties are  $2\sigma$ .



The large RSD (53%) is driven by a subset of samples with relatively depleted  $^{235}\text{U}$  contents, that fall outside of the  $2\sigma$  uncertainty associated with the mean (Fig. 5b). If we apply a  $2\sigma$  outlier rejection, the average  $^{235}\text{U}/^{238}\text{U}$  value of the main population is more precisely defined, with a value of  $0.001677 \pm 0.000030$  ( $2\sigma$ ), which equates to an RSD of 1.8% (Fig. 5c). This is slightly lower, although still within uncertainty of the reference value obtained by LG-SIMS on this material,<sup>18</sup> as presented in Table S3.† The small offset in  $^{235}\text{U}/^{238}\text{U}$  measured by laser ablation is likely to reflect the use of a constant gain factor to correct  $^{235}\text{U}$  measurements on IC2. This technique is sensitive to changes in ion counter performance between analytical sessions that would generate small differences in the  $^{235}\text{U}/^{238}\text{U}$  ratio (see ESI-1† for more details). To overcome this, we recommend use of a secondary glass standard with depleted  $^{235}\text{U}$  contents to calculate the IC2 gain factors during each session. The question of which detector to use for  $^{235}\text{U}$  measurements in an operational scenario is a key consideration. In such a case the isotopic composition of particles will be unknown and potentially have variable  $^{235}\text{U}$  enrichment levels. Samples with high  $^{235}\text{U}$  enrichments are likely to saturate the ion counter, preventing accurate isotope ratios from being attained. Thus, collecting  $^{235}\text{U}$  data on the Faraday detector is the safest and more generalizable option, despite the poor precision for samples with depleted  $^{235}\text{U}$  contents. Future implementation of newly developed amplifiers with  $10^{13} \Omega$  resistors could help to extend the dynamic range of Faraday detectors to the mV-range, *i.e.* decreasing the signal-to-noise ratio for low ion beams. If so, this could be a viable method to ensure percent-level U isotopic data be achieved largely independent of the U isotopic composition of an unknown sample.

The cause of anomalous  $^{235}\text{U}/^{238}\text{U}$  ratios measured with  $^{235}\text{U}$  on the L5 ion counter are difficult to constrain. Unlike U200, where isotopic heterogeneities in  $^{234}\text{U}$ ,  $^{235}\text{U}$  and  $^{236}\text{U}$  covary (Fig. 4a), the heterogeneities in SRNL-DU are only evident in the  $^{235}\text{U}/^{238}\text{U}$  ratio (Fig. 7a). The five DU particles with low  $^{235}\text{U}/^{238}\text{U}$  ratios ( $<0.001$ ) do not have anomalous  $^{234}\text{U}/^{238}\text{U}$  and  $^{236}\text{U}/^{238}\text{U}$  ratios, indicating that the low  $^{235}\text{U}/^{238}\text{U}$  ratios derive from

depletions in  $^{235}\text{U}$ , rather than simple addition of material with high  $^{238}\text{U}$ . Although anomalous  $^{235}\text{U}/^{238}\text{U}$  values could be analytical in origin, it is unclear what process could cause suppression of the  $^{235}\text{U}$  signal during mass spectrometry. Maximum  $^{235}\text{U}$  intensities for SRNL-DU were between 10–20k cps, which are far too low to have caused saturation of the detector or been affected by detector dead time. Although  $^{235}\text{U}/^{238}\text{U}$  ratios were also characterized using the Faraday detectors, the relatively poor precision means we cannot resolve whether similarly anomalous ratios were produced using a different detector. Peak tailing effects from a high  $^{238}\text{U}$  beam would potentially be problematic for a highly  $^{235}\text{U}$ -depleted sample, but this would cause minor isotope ratios to increase and be more prominent on the  $^{236}\text{U}/^{238}\text{U}$  ratio, neither of which are consistent with our observations. The alternative is that the data is accurate and reflects a subset of samples with very low  $^{235}\text{U}/^{238}\text{U}$  ratios within the deposited  $\text{U}_3\text{O}_8$  particle population. However, current analysis of SRNL-DU by LG-SIMS has not identified such a contaminant phase (Scott *et al.* 2021) and would require further characterization of the sample using better imaging techniques and/or secondary ion mass spectrometry (SIMS) for verification. Furthermore, it is difficult to invoke a contaminant phase with an anomalous  $^{235}\text{U}/^{238}\text{U}$  ratio but  $^{234}\text{U}/^{238}\text{U}$  and  $^{236}\text{U}/^{238}\text{U}$  ratios that are identical to the main sample population. Resolving why a subset of U particles have anomalous  $^{235}\text{U}/^{238}\text{U}$  ratios is critical for future implementation of LA-MC-ICP-MS for particle analyses.

The average  $^{234}\text{U}/^{238}\text{U}$  and  $^{236}\text{U}/^{238}\text{U}$  ratios obtained from SRNL-DU particles were  $0.0000071 \pm 0.0000025$  ( $2\sigma$ ) and  $0.000078 \pm 0.000014$  ( $2\sigma$ ) respectively, from 103 measurements (Fig. 6). If a  $2\sigma$  outlier rejection is applied, the final average  $^{234}\text{U}/^{238}\text{U}$  and  $^{236}\text{U}/^{238}\text{U}$  ratios are  $0.0000072 \pm 0.0000018$  ( $2\sigma$ ) and  $0.000079 \pm 0.000010$  ( $2\sigma$ ) from a total of 96 and 95 analyses, respectively. These values equate to external precisions of 25 and 13% respectively for  $^{234}\text{U}/^{238}\text{U}$  and  $^{236}\text{U}/^{238}\text{U}$ . These values are within uncertainty of the reference values obtained using LG-SIMS<sup>18</sup> (Table 4). This indicates that LA-MC-ICP-MS is capable of characterizing abundances of  $^{234}\text{U}$  and  $^{236}\text{U}$  in U particles at the  $<10$  and 80 ppm level, demonstrating that



Fig. 7 Three isotope plots of the uranium composition in SRNL-DU particles with  $^{234}\text{U}/^{238}\text{U}$  vs.  $^{236}\text{U}/^{238}\text{U}$  in (a) and  $^{235}\text{U}/^{238}\text{U}$  vs.  $^{236}\text{U}/^{238}\text{U}$  in (b). Reference values (dashed lines) are from Scott *et al.*<sup>18</sup> All uncertainties are  $2\sigma$ .



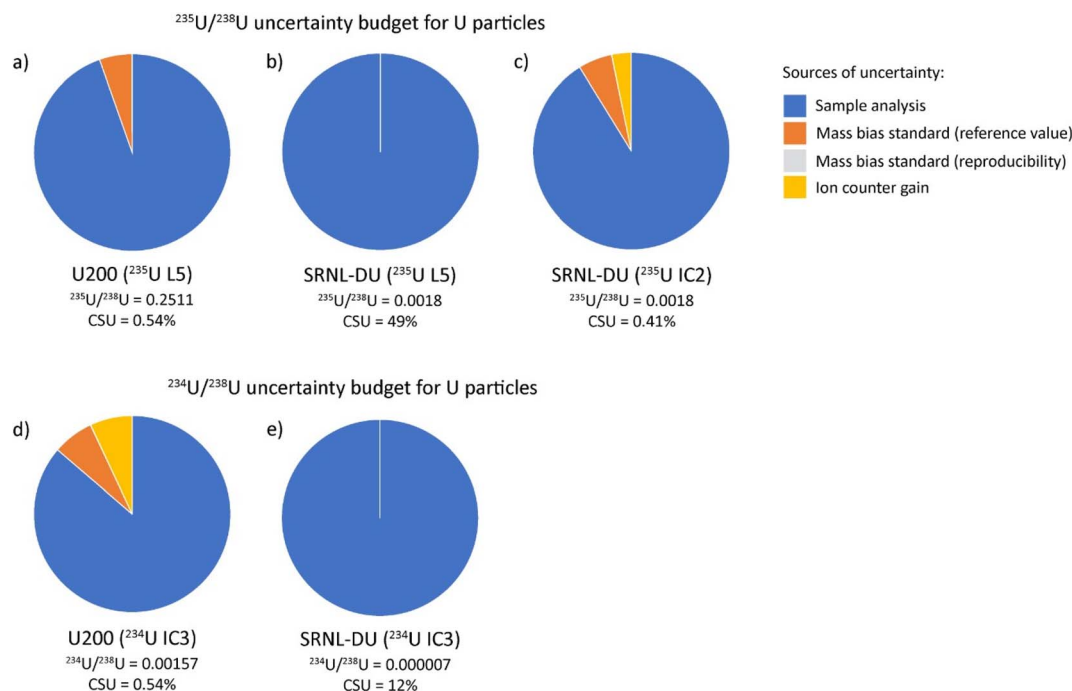


Fig. 8 Uranium isotope uncertainty budgets for the two U particle standards. The uncertainty budgets for  $^{235}\text{U}/^{238}\text{U}$  are provided in (a–c) and uncertainty budgets for  $^{234}\text{U}/^{238}\text{U}$  are provided in (d) and (e). The  $^{234}\text{U}/^{238}\text{U}$  uncertainty budget is largely representative of the budget for  $^{236}\text{U}/^{238}\text{U}$ .

accurate isotopic data can be obtained from count rates in the 10's to 100's of cps.

**3.2.3. Uncertainty budgets.** Typical uncertainty budgets for  $^{235}\text{U}/^{238}\text{U}$  and  $^{234}\text{U}/^{238}\text{U}$  ratios are provided in Fig. 8. Here, the  $^{234}\text{U}/^{238}\text{U}$  uncertainty budget is assumed to be representative of the budget for  $^{236}\text{U}/^{238}\text{U}$ . As shown, the uncertainty budgets for U200 and SRNL-DU are broadly similar, with the dominant source of uncertainty for both  $^{235}\text{U}/^{238}\text{U}$  and  $^{234}\text{U}/^{238}\text{U}$  ratios being the sample analysis itself. This is expected, given the relatively short-lived and highly unstable signal generated by ablation of U particles. Typical CSU values for U200 were between 0.5–2.0% for  $^{235}\text{U}/^{238}\text{U}$  and between 1.0–3.0% for  $^{234}\text{U}/^{238}\text{U}$  and  $^{236}\text{U}/^{238}\text{U}$ . These internal uncertainties are of a similar magnitude to the external precisions (Tables 3 and 4), indicating that the method used to estimate CSU for individual particles is appropriate. For SRNL-DU the CSU values for  $^{235}\text{U}/^{238}\text{U}$  were highly dependent on whether  $^{235}\text{U}$  was measured by Faraday or ion counter. For Faraday measurements, CSU values ranged from 50–200% (due to the significance of the  $^{235}\text{U}$  background subtraction), whereas for ion counter measurements they ranged from 1–2%. For minor isotope ratios, the CSU values were between 10–20% for  $^{234}\text{U}/^{238}\text{U}$  and 3–6% for  $^{236}\text{U}/^{238}\text{U}$ . While significantly larger than the CSU values for U200, this simply reflects the much lower relative abundances of  $^{234}\text{U}$  and  $^{236}\text{U}$  in SRNL-DU (Table S3†). These internal uncertainties are of a similar magnitude to the external precision of  $^{234}\text{U}/^{238}\text{U}$  and  $^{236}\text{U}/^{238}\text{U}$  after outlier exclusion.

### 3.2.4. Data comparison

**3.2.4.1. Laser ablation studies.** Our results show that accurate U isotope data with %-level precision can be obtained for U

particles with significant differences in their isotopic compositions. This is consistent with previous studies that obtained U isotope data with %-level precision from  $\mu\text{m}$  sized particles of natural  $\text{U}^{7,15}$  and the NIST U-oxide standard U050.<sup>15</sup> However, the previous studies investigated a limited range of isotopic compositions and could not adequately investigate the capability to analyze the  $^{236}\text{U}/^{238}\text{U}$  ratio, due to a lack of  $^{236}\text{U}$  in natural U samples. Our current study has increased the range of isotopic compositions that have been successfully characterized by LA-MC-ICP-MS by two orders of magnitude (Fig. 9), including more robust constraints on the  $^{236}\text{U}/^{238}\text{U}$  ratio. Thus, current laser ablation studies have successfully measured the isotopic composition of U-oxide particles with  $^{235}\text{U}$  contents ranging from highly depleted (0.16%) to moderately enriched (25%), which is critical for future use of this technique for characterizing the isotopic composition of U-particles with unknown, but potentially variable, isotopic compositions. One caveat is that current work has focused exclusively on the ability to analyze U in relatively pure substrates, in which U is the dominant component. Particles encountered during environmental testing may have other matrices (e.g. silicates, other metals), within which U is a trace component. As shown from our analyses of U in NIST-610, such materials may be more challenging for accurate isotopic analyses of U by laser ablation, particularly for minor isotope abundances.

**3.2.4.2. SIMS.** On average, the accuracy and precision of U isotope measurements by laser ablation were similar to data obtained by LG-SIMS for the SRNL-DU standard (Table 4). Previous work by Esaka *et al.*<sup>2</sup> analyzed 0.6–4.2  $\mu\text{m}$  particles of U050 by SIMS (IMS-6f) which collected U isotopic data by peak





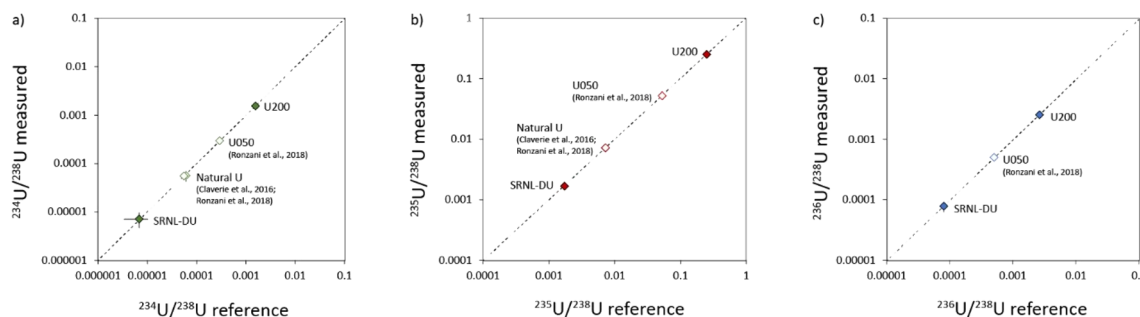


Fig. 9 Comparison between known and measured U isotopic measurements in uranium particles studied here (closed symbols) and in previous studies (open symbols).<sup>7,15</sup> Data for  $^{234}\text{U}/^{238}\text{U}$ ,  $^{235}\text{U}/^{238}\text{U}$  and  $^{236}\text{U}/^{238}\text{U}$  are presented in (a), (b) and (c) respectively. As shown, the analyses of U in SRNL-DU and U200 have greatly increased the range of isotopic compositions that have been characterized in U-particles by LA-MC-ICP-MS.

jumping, in contrast to simultaneous collection by LG-SIMS. Their results showed a strong relationship between isotopic measurement precision and particle size but RSDs associated with the  $^{235}\text{U}/^{238}\text{U}$  ratios of individual particles typically range from 1–2%, which is similar to the laser ablation results (see Tables S5 and S6†). Given that samples for laser ablation have limited sample preparation requirements and isotopic analyses can be performed by rastering over a planchet without prior sample identification or sample characterization, it is clear that LA-MC-ICP-MS can potentially address a niche for rapid isotopic analyses of U particles that is difficult to match by other techniques. A limited comparison of data quality between LA-MC-ICP-MS and SIMS shows that the attained U isotopic data is both accurate and obtained with similar precision (at the %-level).

Although LA-MC-ICP-MS can obtain U isotopic data that matches SIMS for a single particle, we recognize that there are inherent advantages to SIMS that laser ablation cannot match. The first involves the mapping capability of SIMS, which enables an operator to rapidly triage the initial particle population and select individual particles of interest to study in more detail. The second is that SIMS is inherently a less destructive technique than laser ablation, meaning that a particle of interest can be analyzed multiple times if necessary, which might be required if an anomalous isotopic composition is encountered. Because  $\mu\text{m}$ -scale particles are completely consumed during laser ablation, the technique must be thoroughly standardized and have undergone appropriate quality control testing in order to evaluate the isotopic compositions in a sample population with confidence.

## 4. Conclusions

Results of method development and testing at LLNL demonstrate that LA-MC-ICP-MS can achieve accurate U isotope ratio data for silicate glasses and  $\mu\text{m}$  sized U-particles. The results obtained from isotopic analyses of the four silicate glasses demonstrate that LA-MC-ICP-MS can produce U isotopic data that are accurate at the %-level, even for minor isotopes  $^{234}\text{U}$  and  $^{236}\text{U}$ . When operating with %-level precision, effects such as peak tailing and U-hydride formation are not discernible, even

for a sample such as CAS-94-500 which contains  $>90\%$   $^{235}\text{U}$ . However, correction factors for mass bias and ion counter gain remain critical to obtaining accurate data, as typical correction factors shift isotope ratios by several %. The data from NIST-610 illustrate that the chemical composition of the sample analyte is a key consideration, both for trace element content and U isotopic composition.

The ablation of  $\mu\text{m}$  scale U-particles is challenging due to the limited and transient U signal generated by each particle. Despite this, we show that it is possible to achieve accurate and precise  $^{235}\text{U}/^{238}\text{U}$  ratios at the %-level from  $\mu\text{m}$  sized U-particles using LA-MC-ICP-MS. The technique is sufficiently sensitive to produce  $^{234}\text{U}/^{238}\text{U}$  and  $^{236}\text{U}/^{238}\text{U}$  ratios that closely match ratios and uncertainties produced by LG-SIMS. Testing on SRNL-DU demonstrates that  $^{234}\text{U}$  contents  $<10$  ppm and  $^{236}\text{U}$  contents  $<80$  ppm can be resolved in micron-scale particles of uranium. Ultimately, the results of this study indicate that LA-MC-ICP-MS is a promising technique that could be useful in support of the IAEA safeguards verification mission.

## Conflicts of interest

There are no conflicts of interest to declare.

## Acknowledgements

This work was performed under the auspices of the U.S. Department of Energy by Lawrence Livermore National Laboratory under Contract DE-AC52-07NA27344. The work presented in this paper was funded by the National Nuclear Security Administration of the Department of Energy, Office of International Nuclear Safeguards. LLNL-JRNL-841588. Savannah River National Laboratory is managed by Battelle Savannah River Alliance, LLC under Contract No. 89303321CEM000080 with the U.S. Department of Energy. This manuscript has been authored by Lawrence Livermore National Security, LLC under Contract No. DE-AC52-07NA27344 with the US. Department of Energy. The United States Government, and the publisher, by accepting the article for publication, acknowledge that the United States Government retains a non-exclusive, paid-up, irrevocable, world-wide license to publish or reproduce the



published form of this manuscript, or allow others to do so, for United States Government purposes.

## References

- 1 C. Szakal, D. S. Simons, J. D. Fassett and A. J. Fahey, Advances in age-dating of individual uranium particles by large geometry secondary ion mass spectrometry, *Analyst*, 2019, **144**(14), 4219–4232.
- 2 F. Esaka, M. Magara, C. G. Lee, S. Sakurai, S. Usuda and N. Shinohara, Comparison of ICP-MS and SIMS techniques for determining uranium isotope ratios in individual particles, *Talanta*, 2009, **78**(1), 290–294.
- 3 F. Esaka, K. Watanabe, T. Onodera, C. G. Lee, M. Magara, S. Sakurai and S. Usuda, Dependence of the precision of uranium isotope ratio on particle diameter in individual particle analysis with SIMS, *Appl. Surf. Sci.*, 2008, **255**(4), 1512–1515.
- 4 Y. Ranebo, P. M. L. Hedberg, M. J. Whitehouse, K. Ingeneri and S. Littmann, Improved isotopic SIMS measurements of uranium particles for nuclear safeguard purposes, *J. Anal. At. Spectrom.*, 2009, **24**(3), 277–287.
- 5 E. E. Groopman, T. L. Williamson and D. S. Simons, Improved uranium particle analysis by SIMS using  $O_3^-$  primary ions, *J. Anal. At. Spectrom.*, 2022, **37**(10), 2089–2102.
- 6 S. Kappel, S. F. Boulyga and T. Prohaska, Direct uranium isotope ratio analysis of single  $\mu\text{m}$ -sized glass particles, *J. Environ. Radioact.*, 2012, **113**, 8–15.
- 7 F. Claverie, A. Hubert, S. Beraïl, A. Donard, F. Pointurier and C. Pécheyran, Improving Precision and Accuracy of Isotope Ratios from Short Transient Laser Ablation-Multicollector-Inductively Coupled Plasma Mass Spectrometry Signals: Application to  $\mu\text{m}$ -Size Uranium Particles, *Anal. Chem.*, 2016, **88**(8), 4375–4382.
- 8 G. Craig, M. S. Horstwood, H. J. Reid and B. L. Sharp, 'Blind time'-current limitations on laser ablation multi-collector inductively coupled plasma mass spectrometry (LA-MC-ICP-MS) for ultra-transient signal isotope ratio analysis and application to individual sub-micron sized uranium particles, *J. Anal. At. Spectrom.*, 2020, **35**(5), 1011–1021.
- 9 Z. Varga, Application of laser ablation inductively coupled plasma mass spectrometry for the isotopic analysis of single uranium particles, *Anal. Chim. Acta*, 2009, **625**(1), 1–7.
- 10 N. S. Lloyd, R. R. Parrish, M. S. Horstwood and S. R. Chenery, Precise and accurate isotopic analysis of microscopic uranium-oxide grains using LA-MC-ICP-MS, *J. Anal. At. Spectrom.*, 2008, **24**(6), 752–758.
- 11 F. Pointurier, A. C. Pottin and A. Hubert, Application of nanosecond-UV laser ablation-inductively coupled plasma mass spectrometry for the isotopic analysis of single sub- $\mu\text{m}$ -size uranium particles, *Anal. Chem.*, 2011, **83**(20), 7841–7848.
- 12 F. Pointurier, A. Hubert and A. C. Pottin, Performance of laser ablation: quadrupole-based ICP-MS coupling for the analysis of single micrometric uranium particles, *J. Radioanal. Nucl. Chem.*, 2013, **296**(2), 609–616.
- 13 A. Hubert, F. Claverie, C. Pécheyran and F. Pointurier, Measurement of the isotopic composition of uranium  $\mu\text{m}$ -size particles by femtosecond laser ablation-inductively coupled plasma mass spectrometry, *Spectrochim. Acta, Part B*, 2014, **93**, 52–60.
- 14 A. Donard, F. Pointurier, A. C. Pottin, A. Hubert and C. Pécheyran, Determination of the isotopic composition of micrometric uranium particles by UV femtosecond laser ablation coupled with sector-field single-collector ICP-MS, *J. Anal. At. Spectrom.*, 2017, **32**(1), 96–106.
- 15 A. L. Ronzani, A. Hubert, F. Pointurier, O. Marie, N. Clavier, A. C. Humbert and N. Dacheux, Determination of the isotopic composition of single sub- $\mu\text{m}$ -sized uranium particles by laser ablation coupled with multi-collector inductively coupled plasma mass spectrometry, *Rapid Commun. Mass Spectrom.*, 2019, **33**(5), 419–428.
- 16 S. Richter and S. A. Goldberg, Improved techniques for high accuracy isotope ratio measurements of nuclear materials using thermal ionization mass spectrometry, *Int. J. Mass Spectrom.*, 2003, **229**(3), 181–197.
- 17 S. Richter, H. Kühn, Y. Aregbe, M. Hedberg, J. Horta-Domenech, K. Mayer and K. Mathew, Improvements in routine uranium isotope ratio measurements using the modified total evaporation method for multi-collector thermal ionization mass spectrometry, *J. Anal. At. Spectrom.*, 2011, **26**(3), 550–564.
- 18 S. M. Scott, A. T. Baldwin, M. G. Bronikowski, M. A. DeVore II, L. A. Inabinet, W. W. Kuhne and M. S. Wellons, *Scale-up and production of Uranium-Bearing QC reference particulates by an aerosol synthesis method (No. SRNL-STI-2021-00350)*, Savannah River National Lab. (SRNL), Savannah River Site (SRS), Aiken, SC, United States, 2021.
- 19 K. Knight, J. Wimpenny, P. Weber, D. Willingham and E. Groopman, Low-Level Actinide Glasses for Spatial Analyses, *Goldschmidt Abstracts*, 2018, p. 1315.
- 20 G. R. Eppich, J. B. Wimpenny, M. E. Leever, K. B. Knight, I. D. Hutcheon and F. J. Ryerson, *Characterization of Low Concentration Uranium Glass Working Materials (No. LLNL-TR-645481)*, Lawrence Livermore National Lab. (LLNL), Livermore, CA, (United States), 2016.
- 21 E. E. Groopman, D. G. Willingham, A. J. Fahey and K. S. Grabowski, An overview of NRL's NAUTILUS: a combination SIMS-AMS for spatially resolved trace isotope analysis, *J. Anal. At. Spectrom.*, 2020, **35**(3), 600–625.
- 22 R Core Team, *R: A Language and Environment for Statistical Computing*, R Foundation for Statistical Computing, Vienna, Austria, 2021, <https://www.R-project.org/>.
- 23 A. M. Duffin, K. W. Springer, J. D. Ward, K. D. Jarman, J. W. Robinson, M. C. Endres and G. C. Eiden, Femtosecond laser ablation multicollector ICPMS analysis of uranium isotopes in NIST glass, *J. Anal. At. Spectrom.*, 2015, **30**(5), 1100–1107.
- 24 A. M. Duffin, G. L. Hart, R. C. Hanlen and G. C. Eiden, Isotopic analysis of uranium in NIST SRM glass by femtosecond laser ablation MC-ICPMS, *J. Radioanal. Nucl. Chem.*, 2013, **296**(2), 1031–1036.

